

ORIGINAL ARTICLE OPEN ACCESS

The Damhus Hoard: New Insights Into Some of the Earliest Viking Silver Coinage

Thomas Birch^{1,2}  | Helle Horsnæs¹  | Rasmus Andreasen²  | Claus Feveile³  | Stephen Merkel⁴  | Jane Kershaw⁵  | Guillaume Sarah⁶  | Rory Naismith⁷  | Jens Christian Moesgaard⁸

¹National Museum of Denmark, Copenhagen, Denmark | ²Department of Geoscience, Aarhus Universitet, Aarhus, Denmark | ³Museum Vest, Ribe, Denmark | ⁴Earth Sciences, Vrije Universiteit Amsterdam, Amsterdam, the Netherlands | ⁵School of Archaeology, University of Oxford, Oxford, UK | ⁶Institut de Recherches sur les Archéomatériaux – Centre Ernest Babelon, CNRS, Université d'Orléans, Orléans, France | ⁷Department of Anglo-Saxon, Norse and Celtic, University of Cambridge, Cambridge, UK | ⁸Department of Archaeology and Classical Studies, Stockholm University, Stockholm, Sweden

Correspondence: Thomas Birch (thomas.edward.birch@natmus.dk)

Received: 10 July 2025 | **Revised:** 13 May 2026 | **Accepted:** 15 May 2026

ABSTRACT

In 2018, a hoard totalling 266 silver Viking Age coins was discovered near Damhus, south of Ribe (Denmark). The coins belong to the early ninth-century 'KG 4' series, with the vast majority, 262 coins, identified as having Face/Forward Looking Deer on the obverse/reverse. They are among the earliest type of a reformed coinage from Scandinavia's first town, Ribe (Denmark)—some of the first Viking silver pennies. Chemical and lead isotopic analyses of 25 specimens reveal that they are consistent with the admixture of contemporaneous Western (European) silver coinage and the arrival of Eastern silver (homogenised Islamic dirhams) from the first half of the ninth-century. The results indicate that, aside from recycling existing Western silver in circulation, Eastern Islamic silver was being used in Denmark on a major scale from as early as the 820/30s—providing valuable insights into the origins of early Viking Age silver.

1 | Background

The discovery of the Damhus hoard brought to light 266 silver coins belonging to a coinage named by Malmer as 'Kombinationsgruppe 4' (or KG 4) (Malmer 1966; Merkel 2016); 262 of them show a face on one side and an animal on the other (KG 4:1 Face/Forward Looking Deer, see Feveile 2025), and they are thought to date to c. 820/830–850 CE (the remaining four are half pennies showing a ship and a forward looking deer, KG 4:2, see Feveile 2026). The new specimens expand our knowledge and understanding of this particular coin type significantly (Figure 1). Prior to the discovery of the Damhus hoard, only 13 specimens were known of the type Face/Forward Looking Deer (KG4:1), which is in focus in this paper (Moesgaard 2018). The KG 4 series was minted from c. 820/30. Its end-date is not known, but it is likely that it was replaced by the KG 5 coin series around c. 850, meaning its minting can be placed in the first half of the ninth-century.

Although a summary of the Damhus hoard has been published (Moesgaard 2018; Feveile and Moesgaard 2018; Feveile 2021), detailed numismatic publication of the hoard remains ongoing, as is also true of the earlier Series X type pennies. Preliminary die-studies prove the use of many dies and therefore likely a large-scale production of early Viking silver pennies estimated to reach in the 100,000s. The design of the KG 4:1 penny was clearly inspired by that of its predecessor, the Wodan/Monster design from Ribe's earlier silver pennies minted and used as a local monopoly coinage from c. 725 CE until the change to pennies c. 820/830 CE. Although the Series X early pennies are often referred to as *sceattas* (scaet [tas]), the term was not actually used during the period, so the term 'early pennies' is preferred here.

The purpose of this study is to present and contextualise the chemical and isotopic results from the Damhus coins. A detailed overview of the movement and supply of silver in Northern Europe during the Viking Age (and medieval period), including

This is an open access article under the terms of the [Creative Commons Attribution-NonCommercial-NoDerivs](https://creativecommons.org/licenses/by-nc-nd/4.0/) License, which permits use and distribution in any medium, provided the original work is properly cited, the use is non-commercial and no modifications or adaptations are made.

© 2026 The Author(s). *Archaeometry* published by John Wiley & Sons Ltd on behalf of University of Oxford.



FIGURE 1 | Photograph example of KG 4 ‘Damhus type’ silver pennies from the Damhus hoard highlighting the subtle variation, showing a face on one side (‘Wodan’) and a forward looking deer (‘Monster’) on the other, hence also being referred to as the ‘Wodan/monster’ type. They have a maximum diameter of 19.5 mm and weight between 0.8 and 1.25 g (mean = 0.98 g). The coins are (from left to right): x7, x1, x8 and x50, scale (bottom-left) = 10 mm. Photographs by Claus Feveile.

hypothetical models of silver routes, trade and recycling, is not presented here, but can be found in recent publications cited in this article, notably by Kershaw and Merkel (Williams 2007; Skre et al. 2008; Sindbæk 2011; Skre 2011; Merkel 2016; Kershaw et al. 2021; Kershaw and Merkel 2022; Kershaw et al. 2024). The Damhus hoard represents a unique opportunity to investigate and illuminate the source(s) of silver used for minted coinage in southern Scandinavia in the early Viking Age.

2 | Materials and Methods

2.1 | Sampling

Twenty-five pennies (≈10% of the hoard) were randomly selected for sampling for the purpose of chemical and lead isotope analysis. The selected coins are identified individually by their finds number (‘X no’) given to them during the excavation of the hoard; this number is reported in Tables 1 and 3. A sliver of the rim was removed from each using a jeweller’s saw with Antilope jeweller sawblades from Karl Fischer GmbH. Each specimen was mounted individually as a traverse cross-section, embedded in a two-component epoxy resin, prepared as a standard metallographic block, ground using silicon-carbide and flatly polished to a 1- μm finish using diamond paste mediums. The powder (cuttings) obtained from sawing was collected for lead (Pb-)isotope analysis.

2.2 | Analytical Methods

Each mounted specimen (metallographic block) was first analysed for its bulk major and minor elemental composition using

micro-X-ray fluorescence ($\mu\text{-XRF}$) spectroscopy, before being analysed for its trace element composition using laser ablation-inductively coupled-mass spectrometry (LA-ICP-MS). The powder collected from sampling was prepared for Pb-isotope analysis in a Picotrace ultra low particulate (Class 100) metal-free clean laboratory. All sample preparation and analyses were performed at the Department of Geoscience, Aarhus University.

2.2.1 | Micro-XRF

Quantitative data for major, minor and some trace elements were acquired using a Bruker M4 Tornado micro-XRF fluorescence system operating the software module M-Quant (Version 1.5). The X-ray generator was operated at 50 kV high voltage and 600 μA current (Rh X-ray tube). A 20 μm spot size was used (with 20 μm intervals) for chemical analysis (area mapping) of coin samples (dwell time 15 ms/pixel, 3 analytical runs), using an XFlash silicon drift detector simultaneously with the instrument’s second detector for improved counting statistics. This exacted an energy resolution of 40 keV at 130 kcps. Measurements were conducted under 20 mbar vacuum conditions and the acquired spectra evaluated and processed in Bruker’s Esprit software. Within the area mapping, multiple objects (individual analyses) were defined for analysis to monitor coin homogeneity.

Estimations of accuracy and precision are provided by repeat analyses of certified silver-alloy reference materials (133X AGA1, 133X AGA2, 133X AGA3) produced by MBH analytical. They show that the silver bulk can be accurately quantified to within ≈1.5%. The other main elements—Cu, Pb, Zn and Au—are also accurately quantified with errors often less than 5% depending on the concentration. Due to the

TABLE 1 | Micro-XRF results expressed as normalised wt% as the weighted average; *n* = number of areas analysed, area = total analytical area (areas combined) analysed; diff = difference between the surface and core (in wt%). All blanks should be considered below detection limits.

Sample	X no.	n =	Area (µm ²)	Ag	Cu	Pb	Sn	Zn	Au	Fe	Si	Mn	Bi	Ag surface (diff)	Cu surface (diff)
D1	60	4	174,416	92.58	6.02	1.03	0.03	0.09	0.15	0.00	0.07	0.04	0.04	2.83	-3.03
D2	152	8	255,813	93.10	4.75	1.13	0.72	0.72	0.21	0.00	0.00	0.09	0.00	0.12	-0.21
D3	161	4	171,048	94.80	3.76	0.91	0.17	0.02	0.22	0.02	0.21	0.09	0.09	2.30	-1.78
D4	101	3	6428	90.96	6.54	1.75	0.29	0.07	0.07	0.13	0.21	0.05	0.05	2.61	-2.22
D5	33	6	117,097	93.90	4.47	1.15	0.09	0.09	0.24	0.07	0.08	0.00	0.00	2.57	-2.68
D6	163	4	126,893	93.90	4.86	0.92	0.02	0.02	0.19	0.00	0.10	0.00	0.00	0.54	-1.06
D7	84	3	146,854	93.10	5.49	1.09	0.06	0.06	0.15	0.48	0.01	0.10	0.10	1.52	-1.64
D8	105	6	65,143	94.19	3.83	1.14	0.05	0.05	0.23	0.48	0.08	0.00	0.00	-5.26	-2.41
D9	86	3	51,249	92.93	5.21	1.11	0.39	0.12	0.11	0.12	0.12	0.10	0.10	-1.02	-1.90
D10	59	7	167,638	94.95	3.52	1.01	0.12	0.12	0.24	0.05	0.09	0.02	0.02	0.82	-1.24
D11	85	4	124,546	94.10	4.42	1.01	0.04	0.11	0.18	0.04	0.01	0.10	0.00	-2.97	-1.64
D12	5	4	37,674	93.72	4.65	0.88	0.46	0.46	0.22	0.00	0.08	0.08	0.08	1.59	-1.66
D13	42	3	55,525	95.27	3.33	0.98	0.12	0.12	0.21	0.01	0.09	0.08	0.08	0.38	-0.78
D14	91	5	101,298	92.45	5.99	1.15	0.10	0.10	0.12	0.00	0.01	0.08	0.08	2.55	-2.82
D15	57	6	36,662	94.13	4.23	1.11	0.22	0.22	0.09	0.00	0.01	0.08	0.12	0.37	-1.69
D16	29	4	77,448	89.90	8.09	1.14	0.65	0.65	0.14	0.00	0.08	0.00	0.00	4.57	-4.39
D17	96	4	94,765	94.59	3.91	1.03	0.16	0.16	0.22	0.00	0.08	0.08	0.08	0.71	-0.72
D18	25	3	97,895	94.55	3.65	1.02	0.35	0.35	0.26	0.08	0.08	0.00	0.00	-0.29	-2.71
D19	108	4	100,043	94.81	3.47	1.08	0.13	0.10	0.30	0.03	0.07	0.01	0.00	2.64	-2.50
D20	37	4	58,692	92.58	6.09	0.91	0.09	0.09	0.27	0.00	0.06	0.01	0.01	3.09	-2.99
D21	2	4	119,726	93.82	4.62	1.09	0.06	0.13	0.18	0.00	0.09	0.00	0.00	2.47	-2.48
D22	15	3	49,652	93.36	5.12	1.04	0.26	0.26	0.10	0.00	0.08	0.04	0.04	1.48	-1.69
D23	88	4	79,109	94.53	3.82	1.00	0.22	0.22	0.20	0.12	0.01	0.08	0.01	0.20	-0.84
D24	79	3	124,509	92.34	6.07	1.05	0.26	0.26	0.20	0.00	0.08	0.00	0.00	1.79	-2.00
D25	76	7	458,319	93.88	4.15	1.16	0.01	0.51	0.18	0.02	0.09	0.00	0.00	0.62	-0.83
			Min	89.90	3.33	0.88	0.01	0.02	0.07	0.00	0.00	0.00	0.00		

(Continues)

TABLE 1 | (Continued)

Sample	X no.	n =	Area (μm^2)	Ag	Cu	Pb	Sn	Zn	Au	Fe	Si	Mn	Bi	Ag surface (diff)	Cu surface (diff)
			<i>Max</i>	95.27	8.09	1.75	0.17	0.72	0.30	0.48	0.21	0.10	0.12		
			<i>Median</i>	93.88	4.62	1.05	0.06	0.13	0.20	0.04	0.08	0.08	0.00		
			<i>Mean</i>	93.54	4.80	1.08	0.08	0.22	0.19	0.07	0.07	0.06	0.02		
			<i>STDev</i>	1.26	1.16	0.16	0.06	0.19	0.06	0.12	0.05	0.04	0.04		

low concentrations of the standards, accuracy and precision testing of Sn and Bi make error estimations difficult, so LA-ICP-MS data should be consulted. Co, Sb, Cd and As are detected, though values should be treated as qualitative due to their low concentrations. The full results from accuracy and precision testing are shown in Data S1. Accuracy and precision testing of the same silver-alloy standards, as well as other copper-based reference materials, from previous research projects show good long-term consistency and reliability of instrument performance (Birch et al. 2019; Hrnjić et al. 2020; Orfanou et al. 2020; Orfanou et al. 2021).

2.2.2 | LA-ICP-MS

The trace element composition of silver was determined using an Agilent 7900 quadrupole ICP-MS coupled to a RESolution M-50 (ASI) 193 nm ArF excimer laser (ComPexPro 102F, Coherent) system. Calibration of the LA-ICP-MS system was achieved by a continuous ablation of NIST610 at the beginning of each analytical session (two or three times daily), keeping oxide production below 0.25% (monitored as $^{248}\text{ThO}/^{232}\text{Th}$). A total of 28 masses (^{24}Mg , ^{27}Al , ^{48}Ti , ^{53}Cr , ^{55}Mn , ^{57}Fe , ^{59}Co , ^{60}Ni , ^{63}Cu , ^{66}Zn , ^{72}Ge , ^{75}As , ^{77}Se , ^{103}Rh , ^{105}Pd , ^{106}Pd , ^{111}Cd , ^{113}In , ^{114}Cd , ^{113}In , ^{115}In , ^{118}Sn , ^{121}Sb , ^{125}Te , ^{194}Pt , ^{195}Pt , ^{197}Au , ^{208}Pb , ^{209}Bi) was acquired with 15 ms dwell time on each mass during a 551 ms in time resolved—peak hopping—pulse counting/analogue mode. Each ablation constituted a 30s baseline (background) acquisition, 35s sampling (ablation) time and 35s washout. All analyses (coins and standards) were performed over two analytical sessions.

The standard bracketing method was applied, where RM were repeatedly analysed every five sample ablations (before and after every coin); 10 individual ablations were analysed for each coin. The laser settings were: beam diameter of 72 μm , 5 Hz repetition rate, 60 mJ laser energy and 25%T attenuator value. Three silver-alloy RM from MBH analytical (133X AGA1, 133X AGA2, 133X AGA3) were used as standards for quantification purposes of LA-ICP-MS data and for measuring instrument performance (accuracy and precision testing). A value of 95 wt% Ag was used as the internal standard for each coin (individual results can be scaled/re-normalised according to their precise Ag value if needed). Data reduction of time-resolved LA-ICP-MS data was performed using iolite software (Hellstrom et al. 2008; Paton et al. 2011).

Data S2 provides the element concentration (ppm), the standard deviation (2σ) and limits of detection (LOD) for each mass analysed. The results obtained from measuring ^{24}Mg , ^{27}Al , ^{48}Ti , ^{53}Cr , ^{57}Fe , ^{59}Co , ^{60}Ni , ^{72}Ge , ^{77}Se , ^{103}Rh , ^{105}Pd , ^{111}Cd , ^{113}In , ^{194}Pt and ^{195}Pt are not reported in the results section below (though are accessible in Data S2) due to their polyatomic/isobaric interferences (May and Wiedmeyer 1998; Thomas 2002) and/or low accuracy and precision. The full set of results is provided in Data S2.

Quantifying the elemental concentration for each coin followed the same multi-standard trace-element procedure approach outlined previously (Birch, Westner, et al. 2020), namely, taking the median value from three agglomerated datasets (30 values)

corresponding to the compiled results generated by the three silver-alloy RM's used; this was the case for all elements reported here with the exception of the following elements, where the standard(s) used are indicated in brackets: Cu (113X AGA3), Zn (113X AGA1), Au (113X AGA3)—these standards provided values that most closely matched those results obtained independently via micro-XRF analyses.

The results from accuracy and precision testing of RM's are provided in Data S2. They show that the silver-alloy standards are not suitable for the purpose of quantification of pure silver (other RM's), but rather are best suited for trace-element analysis of other impure silver alloys (archaeological). The accuracy and precision performance is inconsistent across three silver-alloy RM's for individual masses (hence adopting a multi-standard element procedure); for 113X AGA1 errors for Co, In, Sn, Te ($\leq 5\%$), Pb and Bi ($\leq 10\%$); for 113X AGA2 errors for Cr, Cu, As, Pd, Cd, In, Sn, Sb, Au and Pb ($\leq 5\%$), Bi ($\leq 10\%$); for 113X AGA3 errors for Pt ($\leq 5\%$), In, Sn, Te, Pb and Bi ($\leq 10\%$). The accuracy and precision results may also owe to micro-inhomogeneity of some elements (nugget effect) in the silver-alloy standards (see Standish et al. 2021).

2.2.3 | Lead Isotopes

Lead isotopes were determined by multi-collector ICP-MS using standard instrumental and chromatographic procedures (Durali-Mueller et al. 2007; Klein et al. 2009). Fresh metal cuttings from the coins were dissolved in Aqua Regia at 110°C in Teflon beakers. Following dissolution, solutions were dried down and passed twice through the column, taken up in 6.0 M HCl (first pass) and then 0.5 M HBr (second pass). These solutions were loaded on Teflon columns containing BioRad AG 1-X8 (200–400 mesh) resin for chromatographic ion exchange separation of Pb using hydrobromic–hydrochloric acid dilutions (cf. White et al. 2000). Following Pb elutions, samples were dried down and the Pb fractions then taken up in 2% HNO₃ with Tl added (single-element standard from PlasmaCal, shown to be isotopically identical to NIST 997 Tl) at a Pb:Tl ratio of $\approx 1:3$ for mass fractionation correction by simultaneously measuring the ²⁰⁵Tl/²⁰³Tl ratio (assuming a ²⁰⁵Tl/²⁰³Tl value of 2.3875 (Rehkämper and Halliday 1998) and exponential law fractionation) and (Pb-isotope ratios for samples and NIST SRM 981 standard). Solutions were analysed on a Nu Plasma II multi-collector ICP-MS equipped with 16 Faraday cups and 5 ion counters in a fixed array, with only Faraday cups used for the measurements with ²⁰⁵Tl as axial mass. Mass 202 and 201 were monitored for Hg interference on mass 204 (²⁰⁴Pb + ²⁰⁴Hg)—which was found to be insignificant. All data were drift-corrected and normalised to NIST SRM 981 (²⁰⁶Pb/²⁰⁴Pb = 16.9406, ²⁰⁷Pb/²⁰⁴Pb = 15.4957 and ²⁰⁸Pb/²⁰⁴Pb = 36.7184).

Two analytical runs (Batch 1 and Batch 2) were performed, each running both samples, standards and a procedural blank (both blanks containing ≤ 1 ng of Pb). Analysis of standard reference materials (geological, lead, silver-alloy) in this study gave constant values of ²⁰⁶Pb/²⁰⁴Pb, ²⁰⁷Pb/²⁰⁴Pb and ²⁰⁸Pb/²⁰⁴Pb ratios within uncertainties of expected values; consistency and

quality of performance from the analysis of standard reference materials using the same analytical procedures and setup can be viewed from previously published data (Birch et al. 2019; Orfanou et al. 2020) and from reference materials analysed in this study (see Data S2).

Pb-isotope ratios measured in artefacts reflect the formation age of the ores and the U, Th and Pb composition of the source from which the ore phases were formed. Pb–Pb model ages have been calculated according to Albarède et al. (2012), using the 'LI_model_age()' function (for use in the R statistical software environment, R Core Team 2026) provided by TerraLID (Westner et al. 2021; formerly the Global Lead Isotope Database, GlobaLID, cf. Klein et al. 2022; Westner et al. 2023; Rose et al. 2024). The Pb-isotope data generated was interpreted from both a geological (cf. Albarède et al. 2012; Pernicka 2017; Tomczyk 2022) and technological (Merkel 2016; Sarah 2018; Kershaw and Merkel 2022; Kershaw et al. 2024) perspective to investigate provenance hypotheses, namely, sources that are most relevant archaeologically, historically and geographically. Where relevant, Pb-isotope data was investigated against published reference data using similar methods and approaches outlined in previous studies (Birch, Westner, et al. 2020; Birch, Kemmers, et al. 2020; Westner et al. 2020).

3 | Results

Based on the results from accuracy and precision testing of the silver-reference materials, the elemental data described below for Ag, Cu, Pb, Zn and Au derive from micro-XRF data, whereas the remainder (As, Sn, Sb, Bi and other trace-elements) derives from LA-ICP-MS data.

The Damhus coins show a relatively homogeneous silver-alloy metal composition containing ≈ 94 wt% Ag with ≈ 5 wt% Cu and ≈ 1 wt% Pb (see Table 1 and Figure 2). The most frequently occurring minor and trace elements from both XRF and LA-ICP-MS analyses are ≈ 0.2 wt% Zn, ≈ 0.2 wt% Sn, ≈ 150 ppm As, ≈ 50 ppm Sb, as well as ≈ 0.2 wt% Au and 500 ppm Bi (see Tables 1 and 2). All other elements, if detected, show median/mean abundances ≤ 5 ppm (i.e., Cd, In, Te). The distribution of elemental composition is shown in Figure 1; the outliers are inconsistent (i.e., do not correspond to the same coin), indicating the compositional range represents the overall variance. Elemental mapping of Ag and Cu (Figure 2) and calculated difference in Ag and Cu values between the core and (coin) surface (see Table 1 and Figure 3) highlight that some coin surfaces have been altered, most likely a result of post-depositional effects (i.e., leaching) as the observed effect is not consistent across all specimens; this serves to highlight and reinforce the importance of analysing 'clean' core metal for defining a representative composition in coin studies (where possible).

The ratios ²⁰⁶Pb/²⁰⁴Pb, ²⁰⁷Pb/²⁰⁴Pb and ²⁰⁸Pb/²⁰⁴Pb are fairly consistent and range between 18.502 and 18.580, 15.656 and 15.671, 38.594 and 38.718, respectively (Table 3). Corresponding Pb–Pb model ages vary between 170 and 217 Ma, that is, the Alpine orogeny.

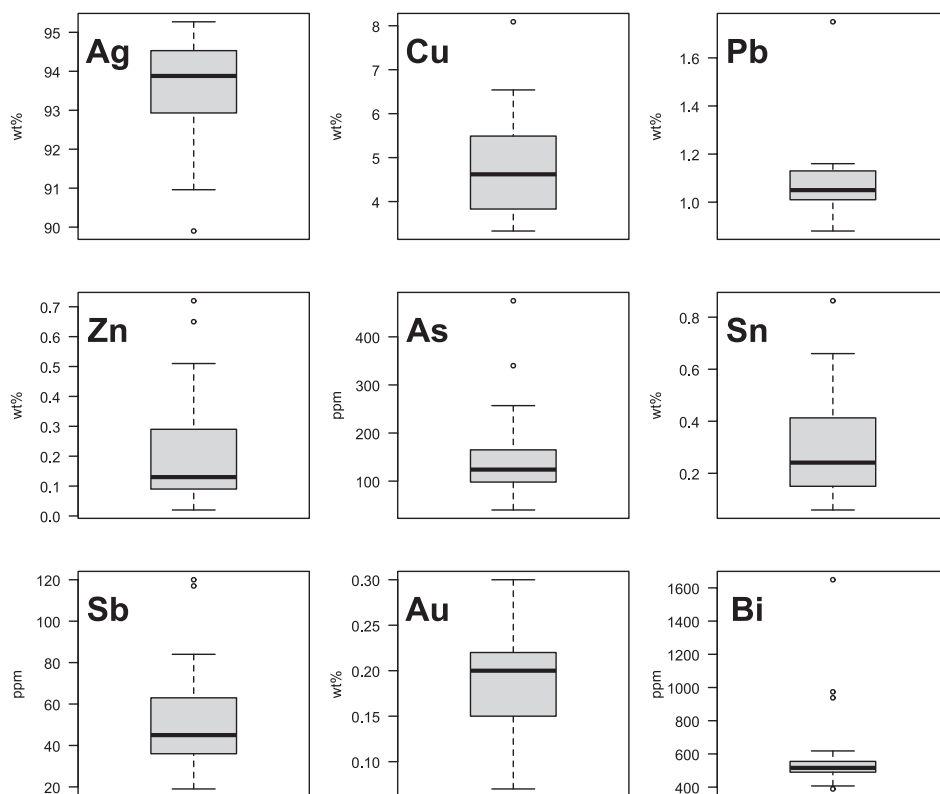


FIGURE 2 | Boxplots showing the relatively homogeneous distribution of elemental compositions for the Damhus coins analysed; three of the 25 coins analysed have notably higher Bi concentrations.

TABLE 2 | LA-ICP-MS results expressed in ppm, each representing the median average from 10 individual ablations across the (unaffected) core of the sample. All blanks should be considered not detected.

Sample	X no.	Cu	Zn	As	Cd	In	Sn	Sb	Te	Au	Pb	Bi
D1	60	64,040	1209	135	1.4	1.8	1650	34	1.8	2815	11,275	938
D2	152	51,370	7091	257	4.0	5.1	4545	84	2.2	7973	10,310	618
D3	161	42,340	274	40	0.6	0.7	601	25	0.6	4646	9125	455
D4	101	38,067	1890	130	2.3	2.7	2365	59	2.3	6658	9485	510
D5	33	47,620	1104	124	2.6	3.6	3215	77	0.5	7206	10,065	477
D6	163	46,560	216	56	1.4	1.8	1500	19	2.0	4087	9100	407
D7	84	54,870	625	108	1.0	1.2	935	23	6.2	3339	10,600	503
D8	105	42,510	650	62	1.5	2.0	1495	38	2.9	5453	10,300	516
D9	86	52,970	2750	141	1.9	2.9	2305	39	2.5	4121	10,520	540
D10	59	36,500	1228	98	2.7	3.3	3085	42	2.3	11,057	8420	429
D11	85	46,920	1344	79	4.9	5.7	5385	43	2.7	3569	10,125	535
D12	5	46,566	4677	193	3.6	4.3	4130	61	2.9	5467	8620	555
D13	42	32,991	1017	55	3.7	4.6	4280	36	2.1	3418	9290	424
D14	91	62,060	4565	340	0.5	1.5	590	117	0.4	5684	11,215	552
D15	57	50,990	2739	165	0.8	1.7	1280	34		5032	10,570	1649
D16	29	51,840	1165	148	5.4	9.2	8630	63	0.8	4272	10,445	508
D17	96	45,450	1454	118	1.3	3.0	2460	120	3.9	9217	9220	490

(Continues)

TABLE 2 | (Continued)

Sample	X no.	Cu	Zn	As	Cd	In	Sn	Sb	Te	Au	Pb	Bi
D18	25	44,600	2737	182	4.3	8.2	6600	84	2.2	29,330	7915	611
D19	108	41,610	1201	121	3.2	5.7	4945	45		10,706	9595	518
D20	37	78,490	1432	215	1.1	2.5	1770	29	8.3	6196	9850	567
D21	2	324,340	1130	104	1.8	2.1	3300	59	2.0	17,200	820	536
D22	15	73,020	8020	475	1.5	2.6	2410	47	2.2	4469	12,150	498
D23	88	49,280	2342	103	1.2	2.6	1855	83	2.5	9301	8085	498
D24	79	52,360	2364	77	0.8	1.5	1160	41	0.5	7655	9355	974
D25	76	45,980	5247	154	1.9	3.5	2500	53	1.2	8702	9665	389
	Min	32,991	216	40	0.5	0.7	590	19	0.4	2815	820	389
	Max	324,340	8020	475	5.4	9.2	8630	120	8.3	29,330	12,150	1649
	Median	47,620	1432	124	1.8	2.7	2410	45	2.2	5684	9665	516
	Mean	60,934	2339	147	2.2	3.3	2920	54	2.4	7503	9445	588
	StDev	55,867	2057	96	1.4	2.1	1963	27	1.8	5567	2059	260

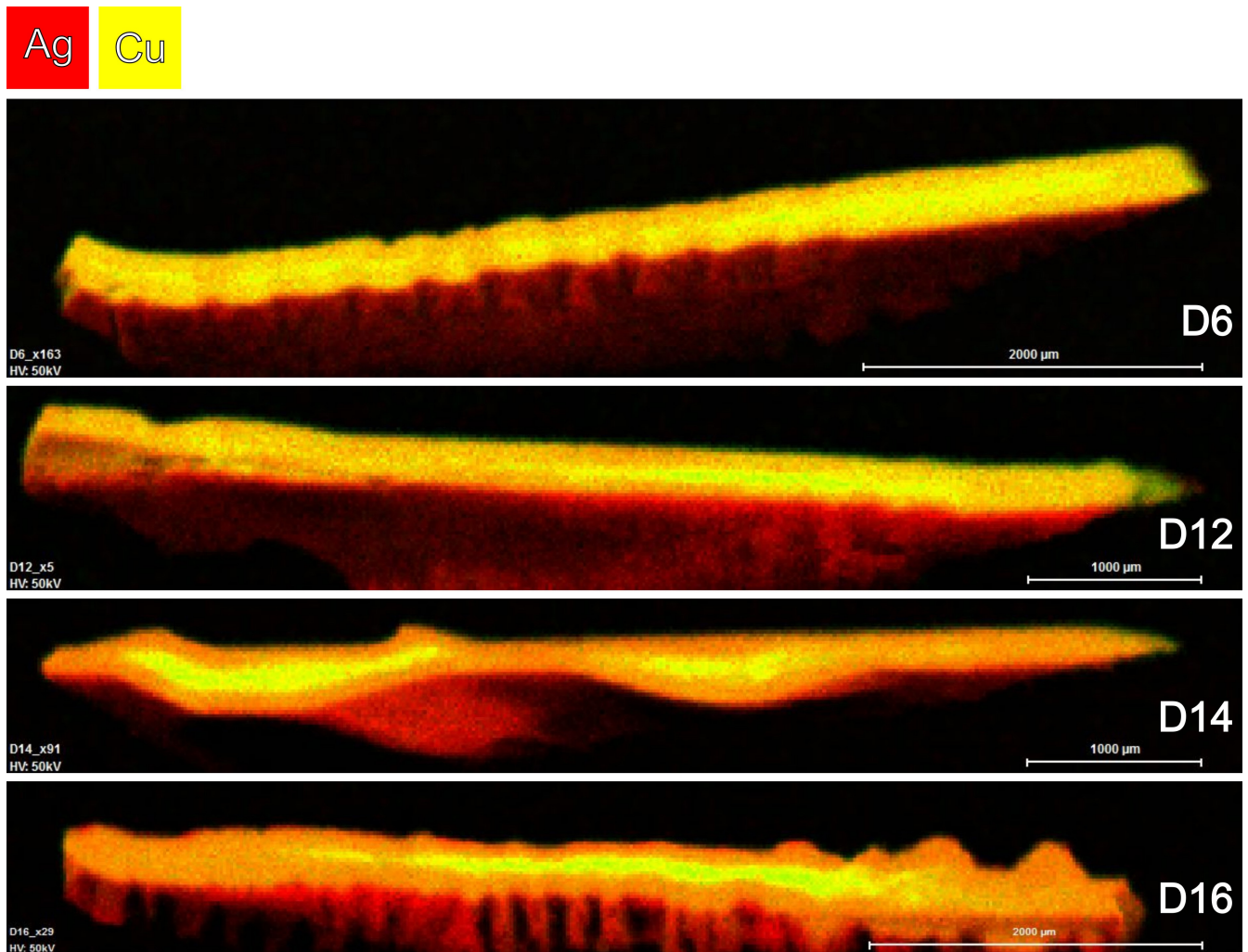


FIGURE 3 | Composite elemental maps showing Ag (red) and Cu (yellow) of several Damhus coins (cross-sections), highlighting the difference between the (affected) coin surface and the (unaffected) coin core; all ablations were performed on the core.

TABLE 3 | Pb-isotope results from MC-ICP-MS, Pb-Pb model ages after Albarède et al. (2012) using the 'LI_model_age()' function provided by TerraLID.

Sample	X no.	$^{208}\text{Pb}/^{206}\text{Pb}$	2σ	$^{207}\text{Pb}/^{206}\text{Pb}$	2σ	$^{206}\text{Pb}/^{204}\text{Pb}$	2σ	$^{207}\text{Pb}/^{204}\text{Pb}$	2σ	$^{208}\text{Pb}/^{204}\text{Pb}$	2σ	T (Ma)	mu	kappa
D1	60	2.08656	0.00015	0.84646	0.00002	18.5020	0.0017	15.6613	0.0017	38.605	0.0049	216	9.746	3.945
D2	152	2.08440	0.00004	0.84522	0.00001	18.5230	0.0003	15.6559	0.0003	38.609	0.0008	195	9.733	3.934
D3	161	2.08427	0.00003	0.84498	0.00001	18.5415	0.0004	15.6671	0.0003	38.645	0.0008	195	9.753	3.942
D4	101	2.08411	0.00011	0.84481	0.00004	18.5374	0.0019	15.6606	0.0024	38.634	0.0064	190	9.740	3.938
D5	33	2.08498	0.00003	0.84520	0.00001	18.5367	0.0004	15.6672	0.0003	38.648	0.0008	199	9.753	3.946
D6	163	2.08374	0.00020	0.84510	0.00003	18.5326	0.0019	15.6618	0.0019	38.617	0.0068	195	9.743	3.933
D7	84	2.08387	0.00004	0.84434	0.00001	18.5543	0.0003	15.6661	0.0003	38.665	0.0008	185	9.749	3.943
D8	105	2.08435	0.00003	0.84481	0.00001	18.5413	0.0003	15.6638	0.0003	38.646	0.0007	192	9.746	3.942
D9	86	2.08470	0.00004	0.84491	0.00001	18.5400	0.0003	15.6646	0.0003	38.650	0.0008	193	9.748	3.944
D10	59	2.08437	0.00014	0.84465	0.00002	18.5445	0.0007	15.6637	0.0009	38.653	0.0024	189	9.746	3.943
D11	85	2.08466	0.00026	0.84489	0.00004	18.5400	0.0011	15.6642	0.0013	38.649	0.0055	193	9.747	3.944
D12	5	2.08380	0.00003	0.84328	0.00001	18.5805	0.0004	15.6687	0.0003	38.718	0.0009	170	9.752	3.952
D13	42	2.08386	0.00015	0.84434	0.00002	18.5453	0.0008	15.6585	0.0007	38.646	0.0028	182	9.735	3.938
D14	91	2.08403	0.00034	0.84432	0.00004	18.5510	0.0011	15.6629	0.0015	38.661	0.0083	184	9.743	3.943
D15	57	2.08722	0.00004	0.84518	0.00001	18.5412	0.0004	15.6706	0.0003	38.700	0.0007	200	9.760	3.967
D16	29	2.08451	0.00005	0.84508	0.00001	18.5329	0.0006	15.6618	0.0006	38.632	0.0020	195	9.743	3.940
D17	96	2.08530	0.00004	0.84642	0.00001	18.5074	0.0004	15.6650	0.0003	38.594	0.0009	217	9.752	3.938
D18	25	2.08383	0.00004	0.84438	0.00001	18.5536	0.0003	15.6661	0.0003	38.662	0.0008	186	9.749	3.942
D19	108	2.08449	0.00007	0.84504	0.00001	18.5368	0.0011	15.6642	0.0010	38.639	0.0026	195	9.747	3.941
D20	37	2.08451	0.00005	0.84442	0.00002	18.5562	0.0004	15.6692	0.0003	38.680	0.0008	188	9.755	3.949
D21	2	2.08428	0.00004	0.84443	0.00001	18.5516	0.0003	15.6653	0.0003	38.666	0.0008	186	9.748	3.945
D22	15	2.08423	0.00004	0.84508	0.00001	18.5356	0.0004	15.6641	0.0003	38.633	0.0008	196	9.747	3.939
D23	88	2.08492	0.00026	0.84542	0.00003	18.5278	0.0007	15.6638	0.0009	38.629	0.0056	201	9.748	3.942
D24	79	2.08598	0.00004	0.84507	0.00001	18.5358	0.0004	15.6640	0.0003	38.665	0.0008	196	9.747	3.953
D25	76	2.08422	0.00007	0.84505	0.00002	18.5358	0.0004	15.6636	0.0004	38.632	0.0011	195	9.746	3.938

4 | Discussion

The discussion here explores the potential and likely sources of silver used to produce the Damhus coins. Having sampled 25 coins, $\approx 10\%$ of the KG4:1 type in the hoard ($n=262$) or 8.6% of those published ($n=291$, Feveile 2025), these results can be considered a representative and robust sample (especially when compared with other studies employing individual objects). The use of ‘high’ Bi and ‘high’ Au is used as a relative term when comparing concentrations of the Damhus coin compositions to the reference data used.

The high Ag content ($\approx 94\text{wt}\%$) of the Damhus coins is directly comparable to silver coinage from the period and region (Sarah 2018; Kershaw et al. 2024). When Sn and Zn are scaled to the Cu concentration, they indicate that impure copper(-alloy) was used to debase the silver, most likely in the form of a low-Sn bronze and/or low-Zn brass.

The Pb-isotope composition of the Damhus coins does not overlap with Scandinavian lead reference data (see Figure in Kershaw and Merkel 2022) and, along with the coins’ relatively consistent Pb concentration ($\approx 1\text{wt}\%$), does not indicate that they were produced from silver refined (i.e., cupellation) by the addition of exogenous lead. It appears most likely that the Damhus coins were produced by re-melting existing silver in circulation, of which the most likely sources are discussed below.

4.1 | Recycling Earlier Silver Coinage c. 660–750

Despite some Pb-isotopic overlaps with earlier Anglo-Saxon, Frisian and Merovingian coinage, they should likely be ruled out as a main contributing source of silver due to the discrepancy in Au and Bi concentrations compared with the Damhus hoard (see Figure 4).

Although some Merovingian silver pennies (namely, those from Tours, cf. Sarah 2018) share similar Au contents to the Damhus coins studied, the vast majority have far higher Au contents (‘high gold’) than Damhus. These earlier high Au pennies are reflective of coinage leading up to Charlemagne’s reform in 793, as shown recently in the chronological development in Au contents of silver pennies (Kershaw et al. 2024). These early silver pennies have Bi concentrations far lower than Damhus, which is enriched in Bi by an order of magnitude.

What remains an unexplored and yet potentially exciting route of silver supply for manufacturing the KG 4 Damhus coin series is the re-melting of earlier Wodan/Monster Series X early pennies (*sceattas*). This precursor coinage, also likely produced in Ribe, provides an obvious route for the re-circulation of silver in the Ribe area of Western Jutland. The chemical and isotopic composition of Series X *sceattas* may relate to and provide further insights on the origins of silver used for minting the Damhus coins; they are currently being investigated as part of an ongoing research project (‘Dark Age Economics’).

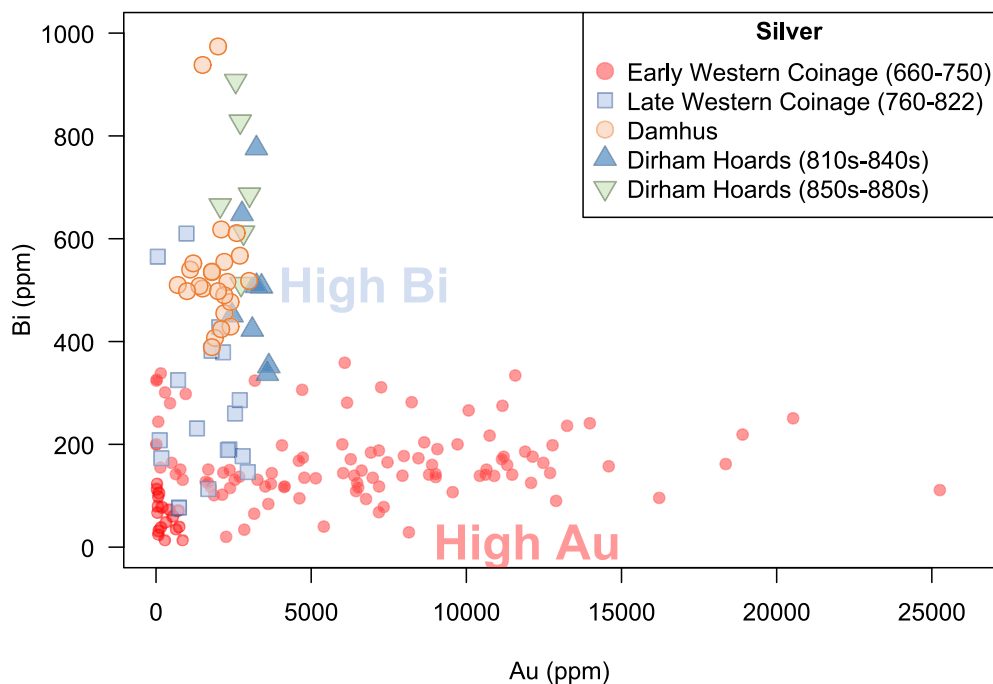


FIGURE 4 | Biplot of gold (Au) and bismuth (Bi) concentrations of the Damhus hoard in comparison with literature data of eighth and ninth-century silver. ‘Early Western Coinage (660-750)’ represents Anglo Saxon and Merovingian (Sarah 2018; Kershaw et al. 2024) coinage from the late seventh to mid-eighth century; ‘Late Western Coinage (760-822)’ represents Anglo Saxon and Carolingian coinage consisting of Anglo-Saxon pennies (Kershaw et al. 2024) from Offa (all 780-92/3, except one coin being 760–780) and Coenwulf of Mercia (797/8-821), as well as Carolingian pennies (Tereygeol et al. 2005; Sarah 2008; Chiarantini et al. 2021; Kershaw et al. 2024) from Charlemagne (793–814) and Louis I Pious (814–822); Damhus represents the analytical results presented in this article; Dirham Hoards (810s–840s) and Dirham Hoards (850s–880s) represents the average composition of ninth-century dirham hoards (Kershaw et al. 2021; Kershaw and Merkel 2022) from the Baltic (all from Gotland, with the exception of one from Oland). The high bismuth (Bi) and high gold (Au) annotations are indications relative to the dirham compositions.

4.2 | Recycling Contemporaneous Western Silver Coinage c. 800–850

The Damhus coin composition is far more consistent with post-793 reform Carolingian silver coinage (Charlemagne and Louis I Pious), sharing a similar range in Au contents (0.1–0.3wt%) as well as overlapping Bi concentrations (see Figures 4 and 5). By the 790s and after, Anglo-Saxon coins were largely made from the same stock of silver as Carolingian coins (Kershaw et al. 2024). The term ‘Western’ silver coinage is used here to refer to this common silver stock used to manufacture both Anglo-Saxon and Carolingian coinage.

The possibility of Carolingian (as well as potentially Anglo-Saxon) silver coinage from the first half of the ninth-century being used to produce the Damhus silver is further reinforced when their Pb-isotope compositions are compared (see Figures 5 and 6). The role of existing Western silver coinage in the formation of the Damhus coin series is also illuminated when considered in conjunction with other available sources of silver, in particular Islamic silver dirhams.

In contrast to the latter, the Damhus gold contents are around 0.1%–0.3%, between post-reform Charlemagne (average 0.1%), Louis the Pious Class 1 and 2 (average 0.17%) and early

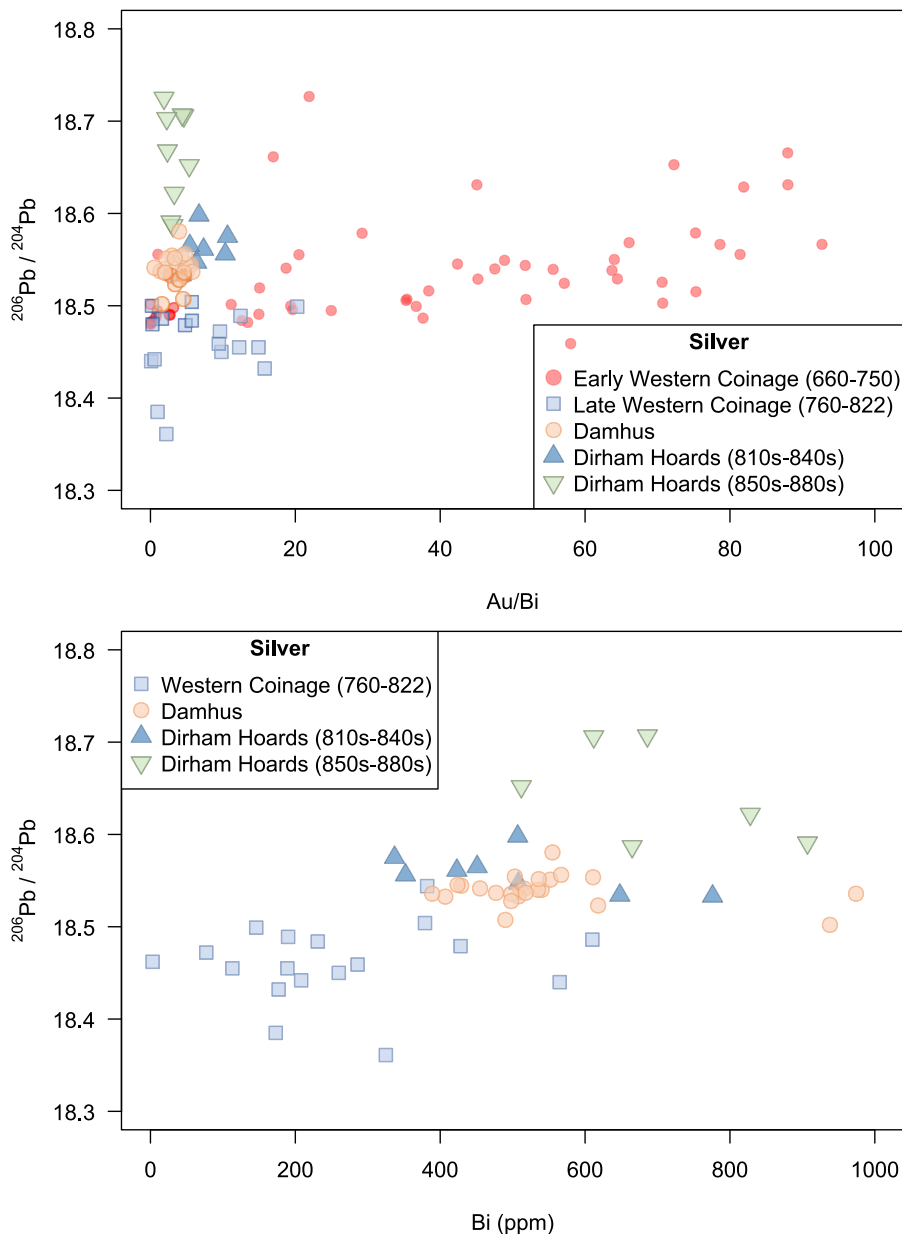


FIGURE 5 | Biplots of Pb-isotope ratio $^{206}\text{Pb}/^{204}\text{Pb}$ against the gold/bismuth ratio (Au/Bi, upper diagram), bismuth (Bi, middle diagram) and gold (Au, lower diagram) concentrations of the investigated Damhus coins in comparison with literature data of eighth and ninth-century silver (reference data as listed in Figure 4 caption); the dirhams have a ‘low’ gold content (<0.5wt% Au) and a ‘high’ bismuth content (>400 ppm Bi) as indicated in Figure 4.

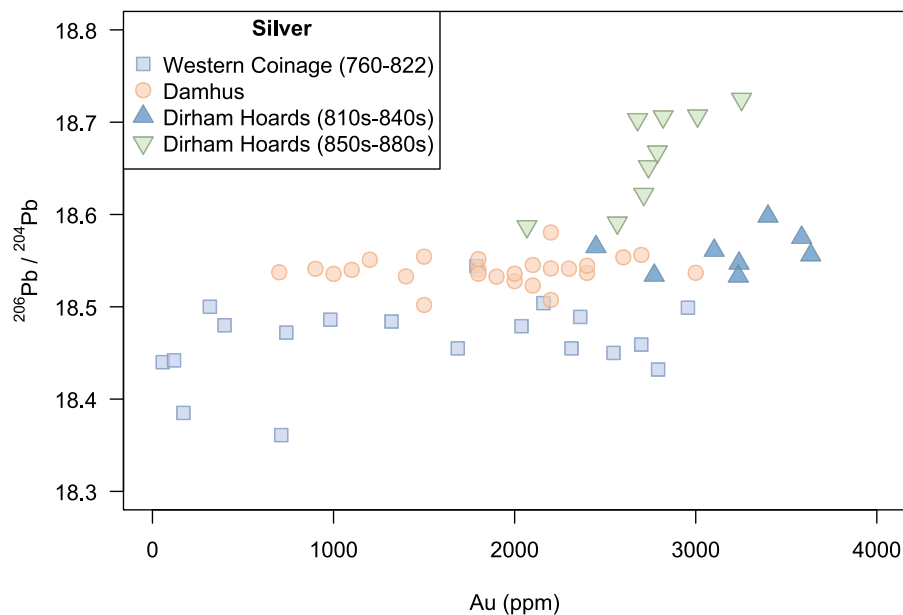


FIGURE 5 | (Continued)

ninth-century Gotland dirham hoard models (0.25%–0.36%); in terms of gold contents, the Damhus hoard straddles between Western silver coinage and (more towards) Islamic dirhams.

Western silver may not have been the only available silver source at the time the Damhus hoard was deposited. Ribe was also in receipt of imports from the Islamic world. This is testified in objects such as beads, as well as silver coin-pendants modelled on Umayyad coins (dirhams): both reached Ribe in the last decades of the eighth century (Sindbæk 2023, 271–279; Feveile 2023, 124). Nevertheless, despite this initial flush, dirhams are not found in later stratigraphic layers at Ribe. More widely in Denmark, dirhams are rare in hoards before c. 850 (Kromann and Roesdahl 1996); two recent hoard finds, Kraneledvej (island of Møn, south-east Zealand) and Skovsholm (Bornholm) each have a *terminus post quem* (tpq) of 848 and 854, respectively (Horsnæs 2023). It is worth mentioning also the slightly earlier hoards containing dirhams from Sønder Kirkeby, Falster (tpq 846/7), and Toftegård, Zealand (tpq c. 850) (Horsnæs 2023).

However, there are indications of the practice of a bullion-weight economy in Ribe, in the form of two polyhedral weights and a piece of hacksilver from ninth-century deposits (Feveile 2023, 130). In addition, the recently discovered Sasanian drachms and early dirhams from Gåbense Vig, Falster, have a preliminary tpq of 829, hinting at an earlier import of Islamic silver than has hitherto been thought to be the case. Recent geochemical work has made the case that dirhams arriving in the Baltic in the mid-ninth century were routinely melted down and cast into rings and ingots, rather than kept as coins (Kershaw et al. 2021).

4.3 | The Introduction of Eastern (Islamic) Silver Dirhams c. 800–850

The massive influx of Islamic silver dirhams to Northern Europe, as well as their re-melting in bulk, is archaeologically

attested (Kilger 2008). Detailed chemical and isotopic studies have determined the geological sources of silver (Merkel 2016; Merkel 2021; Standish et al. 2021; Merkel et al. 2023) and therefore they should be considered as a potential stock source for the Damhus silver, as has already been considered (and demonstrated) for other Viking silver artefacts (Kershaw et al. 2021; Kershaw and Merkel 2022; Kershaw et al. 2025). The reader is pointed in particular to the geochemical and isotopic results from the Viking Age hack-silver hoard Kettilstorp (Västergötland, south-west mainland Sweden), containing both Islamic dirhams (8 Umayyad, 22 Abbasid) and Carolingian coins; not only is the hoard a combination of both Western and Eastern silver, but some of the cast silver pieces directly reflect this admixture (Kershaw and Merkel 2022).

The characteristic Au and Bi contents (≈ 0.2 wt% or less) of ninth-century Islamic silver dirhams (800–900) from important Umayyad and Abbasid mints closely matches the concentrations observed in the Damhus coins. The modelling of chemical and Pb-isotopic compositions of silver dirham hoards found on Gotland and Öland (Kershaw et al. 2021) provides a crucial comparison for the Damhus chemical and Pb-isotope results (see Figure 6). The tightly defined Bi concentration (400–600ppm) of the majority of the Damhus coins (with the exception of the three outliers with substantially higher Bi contents) overlaps well with the modelled Bi contents of the silver dirham hoards from Gotland 800–850. The gold contents of the Damhus coins (ranging from 0.1–0.3 wt%) overlap between the aforementioned Carolingian silver between post-reform Charlemagne (≈ 0.1 wt% Au), Louis the Pious (≈ 0.17 wt% Au, Class 1 and 2) and the modelled gold contents of the dirham hoards from Gotland from the first half of the ninth-century (≈ 0.25 – 0.36 wt% Au).

Overall, the Damhus coins fall neatly between the Western silver coinage from the first half of the ninth-century (i.e., Carolingian pennies) and the modelled (homogenised) compositions from dirham hoards from the same period, both chemically and isotopically. The overall ‘shape’ distribution of the Damhus coins

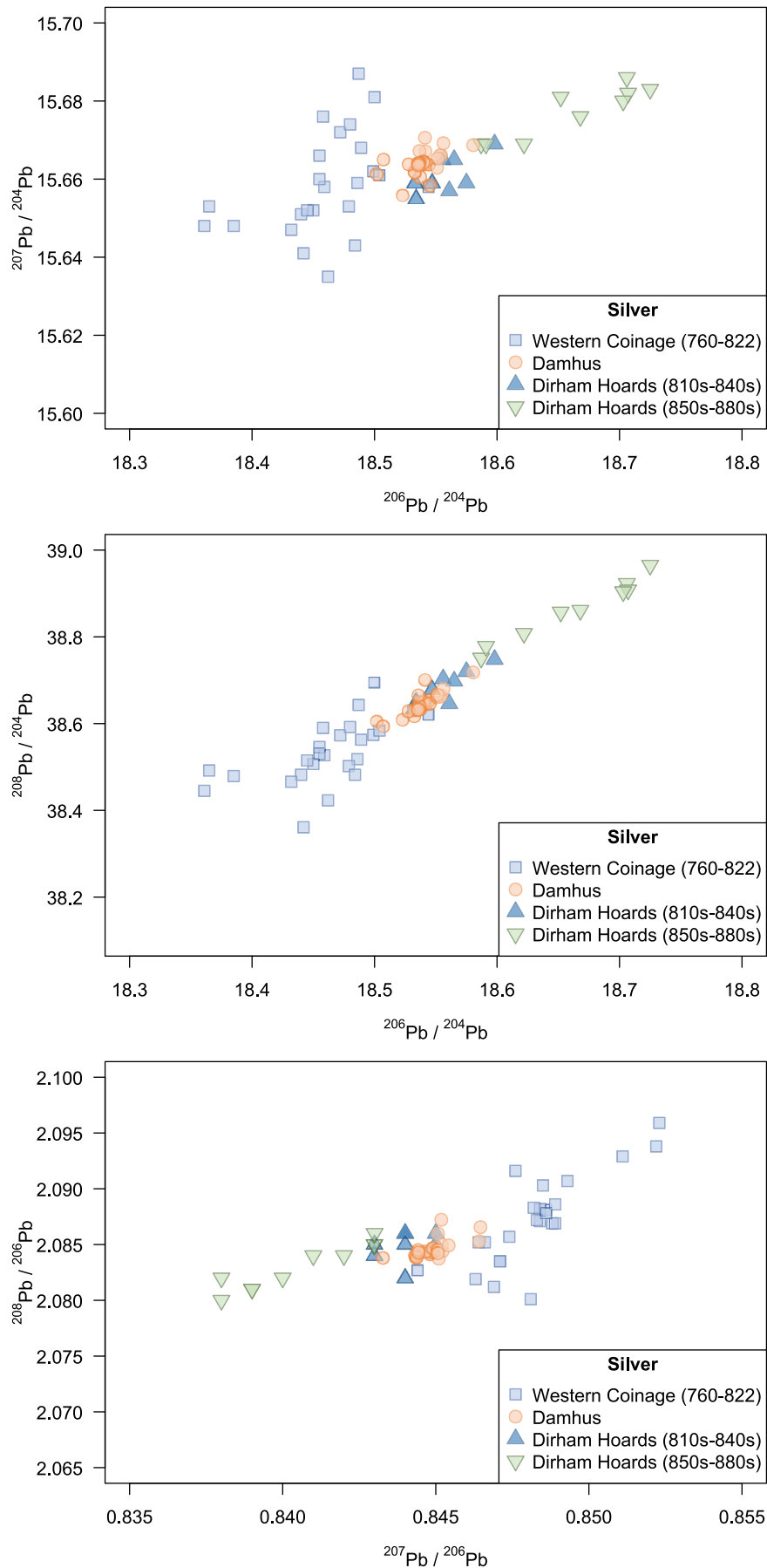


FIGURE 6 | Pb-isotope diagrams of the investigated Damhus coins in comparison with literature data of ninth-century silver, mostly relating to the first half of the ninth-century (reference data as listed in Figure 4 caption).

in the Pb-isotope plots mimics that of the Western silver coinage, but is shifted (scaled and pulled, respectively) towards the Islamic silver hoards. This evidence indicates that silver was being mixed between both anthropogenic (i.e., stock silver metal already available) sources. The proximity of the Damhus Pb-isotope compositions indicates the contributions from silver dirhams to be substantial, as the points are pulled closer to the averaged dirham hoard compositions (away from the Western Carolingian silver). The imported Islamic silver need not have been in the form of coin, but could have arrived in southern Scandinavia as cast bars and ingots.

To add further chronological precision to the dating of the Damhus coins as well as their hypothesised silver origins, they do not match the modelled dirham hoard compositions of the second half of the ninth-century (850–900), as shown in Figure 6, which have distinctly different Pb-isotopic compositions. The three Damhus coins with the highest Bi concentrations (≈ 0.1 – 0.16 wt%) may hint towards being produced in the later part of the first half of the ninth-century (i.e., c. 850) due to their proximity in Pb-isotopes and Bi values to the modelled dirham hoards from 850 to 900. Further investigations and research are needed to understand the relationship between the dating of the Damhus hoard and the numismatic evidence of silver Dirhams in southern Scandinavia.

5 | Conclusion

Although earlier eighth-century silver stocks from Western European coinage have been considered and demonstrated to be an unlikely source of silver for producing the Damhus type KG 4:1 coinage, the Damhus hoard coin compositions and Pb-isotope results fall neatly between (and overlapping with) silver available from the first half of the ninth-century in the form of an admixture of silver pennies (i.e., Carolingian and Anglo-Saxon coinage) and homogenised Islamic (dirham) silver stock in early ninth-century Sweden, as characterised by their Au and Bi contents as well as their Pb-isotopic compositions, similar to the case of the Kettilstorp hack-silver hoard. The results from this study demonstrate that some of the earliest Viking silver coinage was produced by the mixing of existing Western stock silver and newly arriving Eastern Islamic silver. This is significant for showing that Islamic silver was present in southern Scandinavia prior to c. 850, the point at which dirhams first appear in significant number in hoards, and it may be that the silver arrived in the form of cast ingots, bars and rings. Alternatively, the results can be suggestive of a slightly later dating of (some) of the Damhus pennies towards c. 850 (than 830), the point at which the influx of Islamic silver Dirhams is well documented. Whatever the case, the use of Islamic silver for the analysed Damhus hoard coins demonstrates Scandinavia's early connections to long-distance eastern riverine trade networks across Eurasia: even western areas of southern Scandinavia received wealth from trade with the Islamic lands.

Author Contributions

The research project was designed by Horsnæs and Birch, who obtained funding from 'Krogager Fondens og Nationalmuseets Forskningslegat'.

Horsnæs, Feveile and Moesgaard researched the numismatic content. Birch conducted sampling, which was processed by Birch and Andreasen for chemical and isotopic analyses. All authors provided expertise on the analysis, provenance and archaeology of Viking silver. Birch, Horsnæs and Rasmussen prepared the original draft, to which all authors contributed and approved the final manuscript. Reference data was provided prior to and post publication by co-authors Kershaw, Merkel, Naismith and Sarah, which massively aided the interpretation of the Damhus hoard. Merkel significantly improved the original interpretation (Western silver provenance) by comparing the results with the dirham hoards from the Baltic, indicating the early use of Islamic silver dirhams as early as the 820s. The writing up of the manuscript was supported by the Independent Research Fund Denmark (DFR) as part of the project 'Dark Age Economics: the rise of silver, monetisation and cashless currencies in Northern Europe and its relevance for today' (2027-00202B).

Funding

This work was supported by Danmarks Frie Forskningsfond (2027-00202B) and Krogager Fondens og Nationalmuseets Forskningslegat.

Conflicts of Interest

The authors declare no conflicts of interest.

Data Availability Statement

The data that supports the findings of this study are available in the Supporting Information of this article.

Peer Review

For transparency, the peer review documents associated with this article are available at <https://doi.org/10.1111/arc.m.70168>.

References

- Albarède, F., A.-M. Desaulty, and J. Blichert-Toft. 2012. "A Geological Perspective on the Use of Pb Isotopes in Archaeometry." *Archaeometry* 54, no. 5: 853–867.
- Birch, T., F. Kemmers, S. Klein, H.-M. Seitz, and H. E. Höfer. 2020. "Silver for the Greek Colonies: Issues, Analysis and Preliminary Results From a Large-Scale Coin Sampling Project." In *Mines, Metals, and Money: Ancient World Studies in Science, Archaeology and History*, edited by K. A. Sheedy and G. Davis, 101–148. Royal Numismatic Society. Metallurgy in Numismatics 6.
- Birch, T., V. Orfanou, A. Lichtenberger, et al. 2019. "From Nummi Minimi to Fulūs—Small Change and Wider Issues: Characterising Coinage From Gerasa/Jerash Late Roman to Umayyad Periods." *Archaeological and Anthropological Sciences* 11: 5359–5376.
- Birch, T., K. J. Westner, F. Kemmers, S. Klein, H. E. Höfer, and H.-M. Seitz. 2020. "Retracing Magna Graecia's Silver: Coupling Lead Isotopes With a Multi-Standard Trace Element Procedure." *Archaeometry* 62, no. 1: 81–108.
- Chiarantini, L., I. M. Villa, V. Volpi, et al. 2021. "Economic Rebound Versus Imperial Monopoly: Metal Provenance of Early Medieval Coins (9th–11th Centuries) From Some Italian and French Mints." *Journal of Archaeological Science: Reports* 39: 103139.
- Durali-Mueller, S., G. P. Brey, D. Wigg-Wolf, and Y. Lahaye. 2007. "Roman Lead Mining in Germany: Its Origin and Development Through Time Deduced From Lead Isotope Provenance Studies." *Journal of Archaeological Science* 34, no. 10: 1555–1567.
- Feveile, C. 2021. "Damhus-Skatten—En Foreløbig Præsentation af en Ribeudmøntning fra Tidlig 800-Årene." *Arkæologi i Slesvig-Archäologie in Schleswig* 2020, no. 18: 51–66.

- Feveile, C. 2023. "The Numismatic Evidence From Posthustorvet." In *Northern Emporium: Vol. 2 The Networks of Viking-Age Ribe*, edited by S. M. Sindbæk, 115–146. Aarhus University Press.
- Feveile, C. 2025. "Pennies for the King's Towns: Ribe and Haithabu-Pennies From 9th Century." *By, Marsk og Geest—Kulturhistorisk Tidsskrift for Sydvestjylland* 37, no. 1: 5–115.
- Feveile, C. 2026. "KG 4:2 Skib/Fremadskuende Hjort—En Halvpenning fra 800-Årnes Ribe." *Nordisk Numismatisk Unions Medlemsblad* 2026, no. 1: 7–15.
- Feveile, C., and J. C. Moesgaard. 2018. "Appendiks: Damhus-Skatten—Et Fantastisk Indspark til den Tidlige Mønthistorie." *By, Marsk og Geest* 30: 28–30.
- Hellstrom, J., C. Paton, J. Woodhead, and J. Hergt. 2008. "Chapter A9: Iolite: Software for Spatially Resolved LA-(QUAD and MC)-ICP-MS Analysis." In *Laser Ablation ICP-MS in the Earth Sciences: Current Practices and Outstanding Issues*, edited by P. Sylvester. Mineralogical Association of Canada. Vol. 40, 0.
- Horsnæs, H. W. 2023. "The Chosen Few—Sasanian, Arabo-Sasanian and Tabaristani Coins Found in Denmark." In *From Hoard to Archive: Numismatic Discoveries From the Baltic Rim and Beyond Studies in Honour of Ivar Leimus*, edited by E. Russow, V. Dāboliņš, and V. Lang, 79–104. Tartu Ulikooli Kirjastus. Muinasaja teadus 30.
- Hrnjić, M., G. A. Hagen-Peter, T. Birch, G. H. Barfod, S. M. Sindbæk, and C. E. Leshner. 2020. "Non-Destructive Identification of Surface Enrichment and Trace Element Fractionation in Ancient Silver Coins." *Nuclear Instruments and Methods in Physics Research Section B: Beam Interactions With Materials and Atoms* 478: 11–20.
- Kershaw, J., S. Merkel, J. Evans, V. Pashley, and S. Chenery. 2025. "The Provenance of Silver in the Viking-Age Hoard From Bedale." *Archaeometry*: 1–21. <https://doi.org/10.1111/arcm.70031>.
- Kershaw, J., and S. W. Merkel. 2022. "Silver Recycling in the Viking Age: Theoretical and Analytical Approaches." *Archaeometry* 64, no. S1: 116–133. <https://doi.org/10.1111/arcm.12709>.
- Kershaw, J., S. W. Merkel, P. D'Imporzano, and R. Naismith. 2024. "Byzantine Plate and Frankish Mines: The Provenance of Silver in North-West European Coinage During the Long Eighth Century (c. 660–820)." *Antiquity* 98, no. 398: 502–517.
- Kershaw, J., S. W. Merkel, J. Oravisjärvi, E. Kooijman, and M. Kielman-Schmitt. 2021. "The Scale of Dirham Imports to the Baltic in the Ninth Century: New Evidence From Archaeometric Analyses of Early Viking-Age Silver." *Fornvännen* 116, no. 3: 185–204.
- Kilger, C. 2008. "Kaupang From Afar: Aspects of the Interpretation of Dirham Finds in Northern and Eastern Europe Between the Late 8th and Early 10th Centuries." In *Means of Exchange. Dealing With Silver in the Viking Age*, edited by D. Skre, L. Pilø, M. Blackburn, et al., 197–252. Aarhus Universitetsforlag.
- Klein, S., C. Domergue, Y. Lahaye, G. P. Brey, and H.-m.V. Kaenel. 2009. "The Lead and Copper Isotopic Composition of Copper Ores From the Sierra Morena (Spain)." *Journal of Iberian Geology* 35, no. 1: 59–68.
- Klein, S., T. Rose, K. J. Westner, and Y.-K. Hsu. 2022. "From OXALID to GlobaLID: Introducing a Modern and FAIR Lead Isotope Database With an Interactive Application." *Archaeometry* 64, no. 4: 935–950.
- Kromann, A., and E. Roesdahl. 1996. "The Vikings and the Islamic Lands." In *The Arabian Journey: Danish Connections With the Islamic World Over a Thousand Years*, edited by K. von Folsach, T. Lundbæk, and P. Mortensen. Prehistoric Museum Moesgård.
- Malmer, B. 1966. *Nordiska Mynt före år 1000*. Acta Archaeologica Lundensia.
- May, T. W., and R. H. Wiedmeyer. 1998. "A Table of Polyatomic Interferences in ICP-MS." *Atomic Spectroscopy* 19, no. 5: 150–155.
- Merkel, S. 2016. *Silver and the Silver Economy at Hedeby, Veröffentlichungen aus dem Deutschen Bergbau-Museum Bochum Nr. 216*. VML Verlag Marie Leidorf.
- Merkel, S. W. 2021. "Evidence for the Widespread Use of Dry Silver Ore in the Early Islamic Period and Its Implications for the History of Silver Metallurgy." *Journal of Archaeological Science* 135: 105478.
- Merkel, S. W., J. Oravisjärvi, and J. Kershaw. 2023. "Sources of Early Islamic Silver: Lead Isotope Analysis of Dirhams." *Antiquity* 97, no. 396: 1564–1580.
- Moesgaard, J. C. 2018. "Den Fremadskuende Hjort—En Hidtil Uerkendt Fase i Ribes Udmøntning i 800-Tallet?" *By, Marsk og Geest* 30: 17–27.
- Orfanou, V., T. Birch, A. Lichtenberger, et al. 2020. "Copper-Based Metalwork in Roman to Early Islamic Jerash (Jordan): Insights Into Production and Recycling Through Alloy Compositions and Lead Isotopes." *Journal of Archaeological Science: Reports* 33: 102519.
- Orfanou, V., T. Birch, S. M. Sindbæk, C. Feveile, G. H. Barfod, and C. E. Leshner. 2021. "On Diverse Arts: Crucible Metallurgy and the Polymetallic Cycle at Scandinavia's Earliest Viking Town, Ribe (8th–9th c. CE), Denmark." *Archaeological and Anthropological Sciences* 13, no. 5: 81.
- Paton, C., J. Hellstrom, B. Paul, J. Woodhead, and J. Hergt. 2011. "Iolite: Freeware for the Visualisation and Processing of Mass Spectrometric Data." *Journal of Analytical Atomic Spectrometry* 26, no. 12: 2508–2518.
- Pernicka, E. 2017. "Provenance and Recycling of Ancient Silver. A Comment on "Iridium to Provenance Ancient Silver" by Jonathan R. Wood, Michael F. Charlton, Mercedes Murillo-Barroso, Marcos Martínón-Torres. J. Archaeol. Sci. 81, 1–12." *Journal of Archaeological Science* 86: 123–126.
- R Core Team. 2026. *R: A Language and Environment for Statistical Computing*. R Foundation for Statistical Computing.
- Rehkämperab, M., and A. N. Halliday. 1998. "Accuracy and Long-Term Reproducibility of Lead Isotopic Measurements by Multiple-Collector Inductively Coupled Plasma Mass Spectrometry Using an External Method for Correction of Mass Discrimination." *International Journal of Mass Spectrometry* 181, no. 1: 123–133.
- Rose, T., T. Greifelt, K. J. Westner, Y.-K. Hsu, and S. Klein. 2024. "Beteiligung der Fachöffentlichkeit beim Aufbau der Forschungsdateninfrastruktur TerraLID ein Erfahrungsbericht." *Archäologische Informationen* 47: 177–190.
- Sarah, G. 2008. "Caractérisation de la Composition et de la Structure des Alliages Argent-Cuivre par ICP-MS avec Prélèvement par Ablation Laser. Application au Monnayage Carolingien." PhD thesis, Université d'Orléans.
- Sarah, G. 2018. "From Local Supply to Long-Distance Trade Networks: Fingerprinting Early Medieval Silver." In *Silver, Butter, Cloth: Monetary and Social Economies in the Viking Age*, edited by J. Kershaw, G. Williams, S. Sindbæk, and J. Graham-Campbell, 189–205. Oxford University Press.
- Sindbæk, S. M. 2011. "Silver Economies and Social Ties: Long-Distances Interaction, Long-Term Investments—and Why the Viking Age Happened." In *Silver Economies, Monetisation and Society in Scandinavia, AD 800–1100*. 1. oplag. ed. (eds, edited by J. Graham-Campbell, S. M. Sindbæk, and G. Williams, 41–65. University Press.
- Sindbæk, S. M. 2023. "Glass Beads and Beadmaking." In *Northern Emporium: Vol. 2 The Networks of Viking-Age Ribe*, edited by S. M. Sindbæk, 239–281. Aarhus University Press.
- Skre, D. 2011. "Commodity Money, Silver and Coinage in Viking-Age Scandinavia." In *Silver Economies, Monetisation and Society in Scandinavia, AD 800–1100*. 1. oplag. ed. (eds, edited by J. Graham-Campbell, S. M. Sindbæk, and G. Williams, 67–91. University Press.
- Skre, D., L. Pilø, M. Blackburn, et al. 2008. *Means of Exchange. Dealing With Silver in the Viking Age*. Aarhus Universitetsforlag.

- Standish, C. D., S. W. Merkel, Y.-T. Hsieh, and J. Kershaw. 2021. "Simultaneous Lead Isotope Ratio and Gold-Lead-Bismuth Concentration Analysis of Silver by Laser Ablation MC-ICP-MS." *Journal of Archaeological Science* 125: 105299.
- Tereygeol, F., S. Hoelzl, and P. Horn. 2005. "Le Monnayage de Melle au Haut Moyen Age: État de la Recherche." *Association des Archéologues de Poitou-Charentes. Bulletin AAPC* 34: 49–56.
- Thomas, R. 2002. "A Beginner's Guide to ICP-MS Part XII—A Review of Interferences." *Spectroscopy* 17, no. 10: 24–31.
- Tomczyk, C. 2022. "A Database of Lead Isotopic Signatures of Copper and Lead Ores for Europe and the Near East." *Journal of Archaeological Science* 146: 105657.
- Westner, K. J., T. Birch, F. Kemmers, S. Klein, H. E. Höfer, and H.-M. Seitz. 2020. "Rome's Rise to Power. Geochemical Analysis of Silver Coinage From the Western Mediterranean (Fourth to Second Centuries BCE)." *Archaeometry* 62, no. 3: 577–592.
- Westner, K. J., T. Rose, S. Klein, et al. 2023. *GlobalLID—Global Lead Isotope Database (Version 12/2023)*. GFZ Data Services.
- Westner, K. J., T. Rose, S. Klein, and Y.-K. Hsu. 2021. *GlobalLID—Global Lead Isotope Database*. GFZ Data Services.
- White, W. M., F. Albarède, and P. Télouk. 2000. "High-Precision Analysis of Pb Isotope Ratios by Multi-Collector ICP-MS." *Chemical Geology* 167, no. 3: 257–270.
- Williams, G. 2007. "Kingship, Christianity and Coinage: Monetary and Political Perspectives on Silver Economy in the Viking Age." In *Silver Economy in the Viking Age*, edited by J. Graham-Campbell and G. Williams, 177–214. Taylor & Francis Group.

Supporting Information

Additional supporting information can be found online in the Supporting Information section. **Data S1:** Excel workbook containing spreadsheets of: a summary of the results, micro-XRF chemical mapping, micro-XRF results comparing the surface and the core, results from accuracy and precision testing of silver reference materials, Pb-isotope results (individual and repeat measurements) from the Damhus hoard and the analysis of reference materials. **Data S2:** Excel workbook of LA-ICP-MS data containing spreadsheets of: a raw list of compiled LA-ICP-MS data, accuracy and precision results from the analysis of silver reference materials, individual worksheets for each coin (and standard) reporting the full results from the multi-standard element quantification procedure (i.e., compiled results quantified from each analytical standard).